RSC Advances

PAPER

View Article Online
View Journal | View Issue

Cite this: *RSC Adv.*, 2024, **14**, 5875

Tailoring magnetic Sn-MOFs for efficient amoxicillin antibiotic removal through process optimization†

Basmah H. Alshammari,[a] Kaseb D. Alanazi,[a] Omar A. Sheej Ahmad,[b] Sahar Sallam,[c] Amal H. Al-Bagawi,[a] Amal H. Alsehli,[d] Bandar M. Alshammari[a] and Nashwa M. El-Metwaly *[ef]

This study investigated the efficacy of magnetic Sn metal–organic frameworks (MSn-MOFs) in removing the insecticide amoxicillin (AMX) from aqueous solutions. Our thorough experimental investigation showed that MSn-MOFs were an incredibly effective adsorbent for removing AMX. Several methods were used to characterize the material. BET investigation of the data displayed a significant surface area of 880 $m^2\ g^{-1}$ and a strong magnetic force of 89.26 emu g^{-1}. To identify the point of zero charge, surface characterization was carried out and the value was 7.5. This shows that the adsorbent carries a positive and negative charge below and above this position, respectively. Moreover, the impact of pH on adsorption equilibrium was explored. The results of kinetic models to explore the adsorption of AMX on MSn-MOFs supported the pseudo-second-order, and the adsorption complied well with the Langmuir isotherm. The results revealed that the overall adsorption mechanism may entail chemisorption *via* an endothermic spontaneous process with MSn-MOFs. The precise modes by which MSn-MOFs and AMX interacted may involve pore filling, H-bonding, π–π interaction, or electrostatic interaction. Determining the nature of this interaction is essential in understanding the adsorption behavior of the MOFs and optimize the adsorbent design for real-world applications. The use of the MSn-MOF adsorbent provides a straightforward yet efficient method for the filtration of water and treatment of industrial effluents. The results showed 2.75 mmol g^{-1} as the maximum capacity for adsorption at pH = 6. Additional tests were conducted to assess the adsorbent regeneration, and even after more than six cycles, the results demonstrated a high level of efficiency. The adsorption results were enhanced by the application of the Box–Behnken design.

Received 19th December 2023
Accepted 1st February 2024

DOI: 10.1039/d3ra08676c

rsc.li/rsc-advances

1. Introduction

Several variables, such as geographic location, population density, industrial activity, agricultural practices, and healthcare systems, can have a major impact on the amount of antibiotics released into wastewater. Numerous processes, including home sewage, hospital effluents, pharmaceutical production operations, and agricultural runoff, can result in the release of antibiotics into wastewater. Studies have indicated that significant amounts of antibiotics are released into water bodies each year, despite the lack of easily available data on the precise amount of antibiotics discharged into wastewater globally. Antibiotics being dumped into wastewater have raised the alarm due to their potential negative effects on the environment and public health, such as the emergence of antibiotic-resistant bacteria, changes in aquatic ecosystems, and potential hazards to human health from contaminated drinking water.[1] Improved wastewater treatment technology, promoting ethical antibiotic use in healthcare and agriculture, and raising awareness about the possible effects of antibiotic pollution are among the steps taken to reduce the release of antibiotics into wastewater. These steps are crucial for limiting the negative effects of antibiotics on the environment and public health as well as lowering the overall load of antibiotics discharged into wastewater.[2]

Several factors make it essential to remove pharmaceuticals from wastewater: pharmaceuticals can harm aquatic life when they are released into water sources, which can have an

[a]*Department of Chemistry, College of Science, University of Ha'il, 81442, Ha'il, KSA*
[b]*Department of Chemistry, College of Education for Pure Sciences, University of Mosul, Iraq*
[c]*Department of Chemistry, Faculty of Science, Jazan University, Jazan, P. O. 45142, Saudi Arabia*
[d]*Chemistry Department, College of Science, Taibah University, Madinah 42353, KSA*
[e]*Department of Chemistry, Collage of Sciences, Umm Al-Qura University, Makkah, Saudi Arabia. E-mail: nmmohamed@uqu.edu.sa*
[f]*Department of Chemistry, Faculty of Science, Mansoura University, El-Gomhoria Street 35516, Egypt. E-mail: n_elmetwaly00@yahoo.com*

† Electronic supplementary information (ESI) available. See DOI: https://doi.org/10.1039/d3ra08676c

influence on the environment. They can interfere with the endocrine systems of various organisms even at low concentrations, thus having negative effects on the entire ecosystem. Pharmaceutical residues in water sources have the potential to enter drinking water systems, raising implications for human health. Even at modest doses, prolonged exposure to these compounds may harm human health, resulting in antibiotic resistance, hormone abnormalities, and other unanticipated effects. Drugs in wastewater have the potential to upset the harmony of microbes and other living forms that are crucial to the upkeep of a healthy ecosystem. This could have a number of effects, including altered nutrient cycling and disturbed food chains. Antibiotic-resistant bacteria can evolve as a result of environmental exposure to medications, which could eventually cause a public health emergency.[3,4] The development and spread of antibiotic resistance can be slowed down with the proper removal of these chemicals from wastewater. Strict laws for regulation compliance against the disposal of medications into water bodies are in place in several nations. To guarantee adherence to rules and regulations governing environmental protection, toxic chemicals must be effectively removed. Pharmaceuticals are removed from wastewater before they are back in the environment using a variety of technologies, such as membrane filtering, activated carbon adsorption, sophisticated oxidation procedures, and biological treatment methods. Additionally, minimizing the amount of pharmaceuticals in wastewater can be significantly helped by public awareness campaigns and ethical disposal techniques.[5–7] The environment, people's health, and ecological systems are all at risk when there are leftover antibiotics in wastewater. Among the major dangers are antibiotic resistance; one of the biggest worries is the possible emergence and spread of microorganisms that are resistant to antibiotics. Low quantities of antibiotics in wastewater can provide a selective environment that encourages the emergence of resistant strains, which pose a serious threat to both human and animal health. Ecosystem-disturbing antibiotics have the potential to upset the normal equilibrium of microbial populations in soil, water, and sediment. This disruption may impair the cycling of nutrients, deteriorate water quality, and promote the growth of some species at the expense of others, damaging the ecological balance as a whole. Aquatic life harm: fish, amphibians, and invertebrates living in water can be poisoned by antibiotic residue in wastewater.[8–11] These compounds have the potential to disrupt a variety of physiological systems, impair reproductive behavior, and induce developmental defects even at low concentrations, ultimately resulting in population decrease and ecological imbalances. Consequences for human health: antibiotics in wastewater have the potential to pollute sources of drinking water, exposing people unintentionally.[12,13] Long-term low-dose antibiotic exposure may have other unidentified health impacts in addition to contributing to the development of antibiotic-resistant diseases. Environmental persistence: some antibiotics have the potential to linger in the environment for lengthy periods of time, posing dangers to ecosystems and human populations alike. Their persistence may also cause these compounds to build up in diverse environmental spaces, thereby worsening their long-term effects. Implementing efficient wastewater treatment systems that focus on the removal of antibiotics is crucial to reducing these concerns. A further way to lessen the overall burden of antibiotics entering wastewater systems is to encourage their safe use in healthcare, agriculture, and aquaculture. In order to successfully manage these concerns, monitoring and controlling the entry of antibiotics into the environment is also essential.[14,15]

The common antibiotic amoxicillin may be successfully removed from wastewater by means of a variety of treatment methods. One of the most popular techniques for its removal is adsorption. Adsorption is a technique by which molecules cling to the surface of a solid substance. Using the adsorption method to extract amoxicillin using wastewater has the following advantages.[16–18] Great effectiveness: amoxicillin may be removed from water using adsorption procedures with high removal efficiencies, guaranteeing that the antibiotic concentration is decreased to safe limits. Adsorption techniques are frequently inexpensive, especially when compared to other cutting-edge treatment options. Adsorption materials are often inexpensive, and the procedure is simple to incorporate into already-existing wastewater treatment systems. Adsorption is a flexible and versatile method for removing amoxicillin from a variety of sources, such as pharmaceutical industrial effluents, hospital wastewater, and agricultural runoff. It can be applied to varied wastewater streams. Simple operation and upkeep adsorption systems require little setup or maintenance.[19] It is simple to regenerate or replace the adsorbent material once it has been saturated with amoxicillin, enabling continued and effective treatment. Adsorption methods typically do not leave behind any hazardous byproducts or residues, reducing the treatment's negative environmental effects.[20] The adsorbent materials can be securely disposed of or recovered for reuse, minimizing their overall environmental impact.[21] Amoxicillin can be successfully removed from wastewater using a variety of adsorbent materials, such as activated carbon, zeolites, and different modified natural and manmade materials.[22] These substances are effective at removing the target antibiotic because of their high surface areas and particular affinity for it. To ensure that amoxicillin and other medicines are successfully removed from wastewater before it is discharged into the environment, adsorption can be used as a standalone treatment method or as a phase in a multi-step treatment process. Regarding the adsorption and elimination of amoxicillin from wastewater, magnetic metal–organic frameworks (MOFs) offer a number of advantages over traditional adsorption techniques. Several of these benefits include high porosity and wide surface areas, which are typical characteristics of magnetic MOFs and enable them to have a higher adsorption capacity than many other adsorbents.[23] This means that even at low concentrations, amoxicillin can be effectively removed from wastewater. In addition, by applying an external magnetic field, these MOFs can be effortlessly separated from the aqueous matrix thanks to their magnetic characteristics. This makes the procedure more affordable and sustainable by enabling the recovery and use of the adsorbent material. Due to their fast adsorption kinetics, magnetic MOFs may quickly remove amoxicillin from

wastewater in a short amount of time, making the procedure quicker and more suitable for large-scale applications. Magnetic MOFs can be recycled and utilized repeatedly without suffering a major reduction in their adsorption capacity. Compared to some other adsorbent materials that may need frequent replacement, their reusability feature makes them more commercially and environmentally viable. They have surface functionalities that can be tailored as desired. To increase their selectivity and affinity for particular target substances like amoxicillin, the surface characteristics of magnetic MOFs can be altered or functionalized.[24] This degree of adaptability enables the creation of extremely effective adsorbents that cater to particular requirements for wastewater treatment. Also, when exposed to a variety of environmental factors, such as changing pH levels and temperatures, magnetic MOFs are stable and durable, thus ensuring their longevity and long-term performance in wastewater treatment applications. The usage of magnetic MOFs in the adsorption and removal of amoxicillin from wastewater can considerably increase the efficiency, sustainability, and cost-effectiveness of the treatment process by taking advantage of these benefits, thus helping to preserve the environment besides public health as a whole.[25]

2. Experimental

2.1. Synthesis of Fe_3O_4

In the solvothermal process, $FeCl_3 \cdot 6H_2O$, sodium acetate, and sodium citrate were combined with ethylene glycol as the solvent to produce Fe_3O_4 nanoparticles (NPs). The procedure consists of multiple stages. First, 1.14 g of $FeCl_3 \cdot 6H_2O$, 2.4 g of sodium acetate, and 0.65 g of sodium citrate in 50 mL of ethylene glycol were mixed and agitated for 30 minutes at 25 °C until they created a uniform solution. Afterward, the solution was heated. The mixture was heated to 200 °C for 10 h in an autoclave sealed with Teflon. The application of high temperature and pressure within the autoclave encourages the synthesis of Fe_3O_4 nanoparticles. Following the completion of the reaction, the Fe_3O_4 nanoparticles were extracted from the solvent with the aid of a magnet owing to their magnetic nature. Subsequently, to get rid of any contaminants that may still be present, the separated NPs were washed numerous times with deionized water and alcohol. The NPs are next dried in a vacuum at room temperature to remove any last traces of moisture.[7]

2.2. Synthesis of Fe_3O_4@Sn-MOF (MSn-MOF)

Initiating the reaction process involved introducing a 4 mL solution of Fe_3O_4 nanoparticles (0.25 mg mL^{-1}) into a mixture containing 2-methylimidazole (Hmim) in methanol (0.82 g) with a total volume of 26 mL. Ultrasonication was applied for 15 minutes to ensure thorough mixing. Following this, 2.275 g (0.012 moles) of $SnCl_2$ was added, then the mixture was left at room temperature for a duration of 2 h without stirring. The final steps included a methanol wash and magnetic separation of the product (Fig. 1).[9]

2.3. Batch studies of MSn-MOF

To eliminate AMX, a conventional batch adsorption procedure was employed. Firstly, the AMX concentration used for equilibrium besides kinetic adsorption was 2.6×10^{-3} mol L^{-1}. Additionally, different dosages of the adsorbent ranging from 0.01 to 0.25 g/25 mL at temperatures from 293 to 323 K and for varying time periods from 5 to 100 minutes were used.[10] To evaluate the effect of pH on adsorption, we examined a pH series from 2 to 12 using either acidic (0.1 mol L^{-1} of HCl) or alkaline (0.1 mol L^{-1} of NaOH) solutions as constant limits. We also looked at the properties of thermodynamic adsorption at 293, 303, and 333 K. We used an UV-vis spectrophotometer to analyze the adsorption process. Further assessments were carried out to investigate factors such as ionic strength, the original concentration of amoxicillin, adsorbent dosage, and recyclability. In order to determine the rate of removal (percent R) and the equilibrium capacity for adsorption (q_e), the global

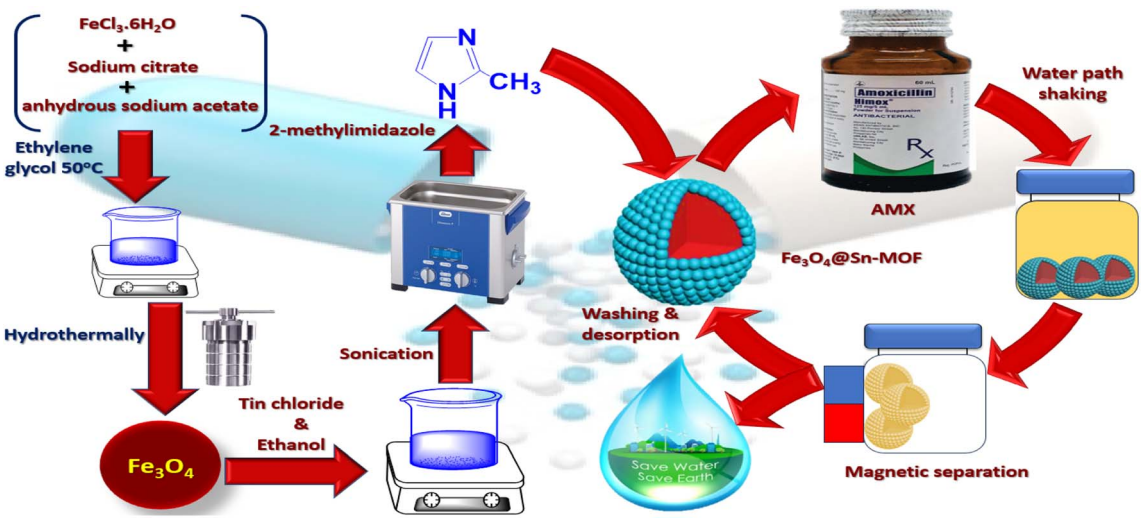

Fig. 1 Diagram showing the elimination of AMX and the synthesis of MSn-MOFs.

mass distribution of AMX particles in the batch was utilized in conjunction with eqn (1) and (2).

$$\% R = \frac{(C_0 - C_t)}{C_0} \times 100 \quad (1)$$

$$q_e = \frac{(C_0 - C_e)V}{M} \quad (2)$$

In the equations, C_0 represents the initial concentration of AMX, C_e signifies the equilibrium concentration, V characterizes the solution volume, and m signifies the mass of the MSn-MOF material. These equations enable the assessment of the adsorption capacity (q_e) and the efficacy of AMX removal (% R) achieved by the MSn-MOF material.

3. Results and discussion

3.1. Characterization of MSn-MOF

The primary goal of XRD patterns is to identify the hypothesized construction of MSn-MOF and to take other information on its structure into consideration.[26] The synthesized MSn-MOFs' structural integrity was inspected by means of XRD. The XRD patterns of MSn-MOF developed in the 5–80° scan range are displayed in Fig. 2(a). The XRD patterns of Sn-MOF demonstrated strong and sharp peaks at 2θ of 14.79°, 15.76°, 25.088°, 26.8°, 29.7°, 31.64°, 56.22°, 56.22°, 61.06° and 61.74°, suggesting a high crystallinity level. Sn and Fe ions were coordinated by Hmim anions utilizing surface complexation to give MSn-MOF its high degree of crystallinity. The produced Fe_3O_4@Sn-MOF displayed intense crystalline peaks at 2 values less than 25.088°, as illustrated in Fig. 2(a). These computations also allowed for the determination of crystallinity as $a = 14.18$ Å, $b = 11.21$ Å, $c = 1.65$ Å, $\alpha = 90°$, $\beta = 90°$, $\gamma = 90°$. Table S1 (ESI)† displays the MSn-MOF's Miller indices (hkl) with interplanar spacing (d_{hkl}). The fact that the diffraction peaks of the MSn-MOF were preserved during adsorption is another indication from our data that their crystal structure is fairly strong.[27]

The Brunauer–Emmett–Teller (BET) method was used to calculate the samples' nitrogen adsorption–desorption isotherm at 77 K as well as their porosity and surface area. Utilizing the BET formula, the specimen's surface area as well as pore size distribution were determined (Fig. 2(b)). It was found that MSn-MOF and AMX@MSn-MOF each have high surface areas of 880 $m^2\ g^{-1}$ and 532.6 $m^2\ g^{-1}$, respectively. Materials with high porosity that correspond to the size of the pore radius have been found to exist. The NLDFT approach was utilized to ascertain the appropriate distribution of pores in the substance by calculating the pore size distribution for Sn-MOF that has a large surface area of 922 $m^2\ g^{-1}$. The half-pore width measured by DFT (Density Functional Theory) was determined. MSn-MOF (Mesostructured Material) is close to a mesoporous substance owing to its 2.6 nm pore size and 1.04 $cm^3\ g^{-1}$ pore volume. The pore volume reduced to 0.72 $cm^3\ g^{-1}$ when amoxicillin was adsorbed on MSn-MOF, indicating conclusively that a part of the AMX was absorbed by the pore structure. MSn-MOF demonstrates a type II isotherm and displays numerous mesopores within the model. To remove AMX from aqueous solutions, a mesoporous structure having a large specific surface area could prove to be helpful.[10,18]

SEM was employed to explain the shape of the produced MSn-MOF powder, and a higher magnification micrograph is shown in Fig. 2(c). The characteristic nanoparticle morphology with sizes ranging from 150 to 200 nm was visible in the FE-SEM scans.

Fig. 2(d) shows the FTIR spectra of MSn-MOFs before and after AMX adsorption. The MSn-MOF spectrum has extra peaks that are revealed by the FTIR investigation.[28] In particularly, the stretching vibration of O–H bonds is linked to the large peak detected at 3377.1 cm^{-1}, demonstrating that MSn-MOF contains hydroxyl groups. The stretching vibration of C=N bonds is responsible for another peak at 1621.8 cm^{-1}, indicating that the MSn-MOF structure contains amino groups. These different peaks throw light on the material's chemical composition and characteristics by offering essential information about the functional groups existing in the model. The FTIR spectra give us further information about the structure and functional groups of MSn-MOF both before and after AMX adsorption. Here is a summary of the findings: peaks at 2915.84 and 2973 cm^{-1} are accredited to the stretching vibrations of $-CH_3$ and $-CH_2$, respectively. These peaks imply that the MSn-MOF has become functionalized. The asymmetric vibration of C–O in the MSn-MOF is represented by the peak seen at 960.37 cm^{-1}, which indicates that this functional group is present. The FTIR spectra show that different functional groups, like hydroxyl, carboxyl, and amino groups, are involved in the adsorption of AMX on the MSn-MOF. The FTIR spectra show that different functional groups, such as (O–H, C=N), are involved in the adsorption of AMX on the MSn-MOF. These changes are a result of the adsorption process, which causes changes in the chemical environment. A comprehensive analysis of the observed alterations in the functional groups offers a more thorough breakdown of the FTIR measurements carried out prior to and following AMX adsorption and the peak heights that go with them.[29,30]

Fig. 2(e) shows that the saturation of magnetization (M_s) value of Fe_3O_4 nanoparticles and MSn-MOF at room temperature is 135.9 and 89.26 emu g^{-1}, individually. Owing to their special qualities, these materials make good magnetic adsorbents that can be separated from the adsorption process with ease using a simple magnetic field, thus negating the need for centrifugation.[31,32]

Utilizing X-ray photoelectron spectroscopy (XPS), the chemical composition and binding energy of the artificial MSn-MOF composite sponge were examined.[31,33] According to Fig. 3, the synthetic MSn-MOF composite sponge's XPS pattern shows unique peaks at particular binding energies of 284.9, 530.7, 400.6, 485 and 710 eV, which represent carbon, oxygen, nitrogen, tin and iron, respectively. These XPS peaks offer useful information regarding the elemental makeup and chemical environments of the composite sponge.[34–36]

3.2. Batch research

3.2.1. Influence of pH upon zero charge point. The adsorbent's point of zero charge (PZC) and the pK_a values of AMX

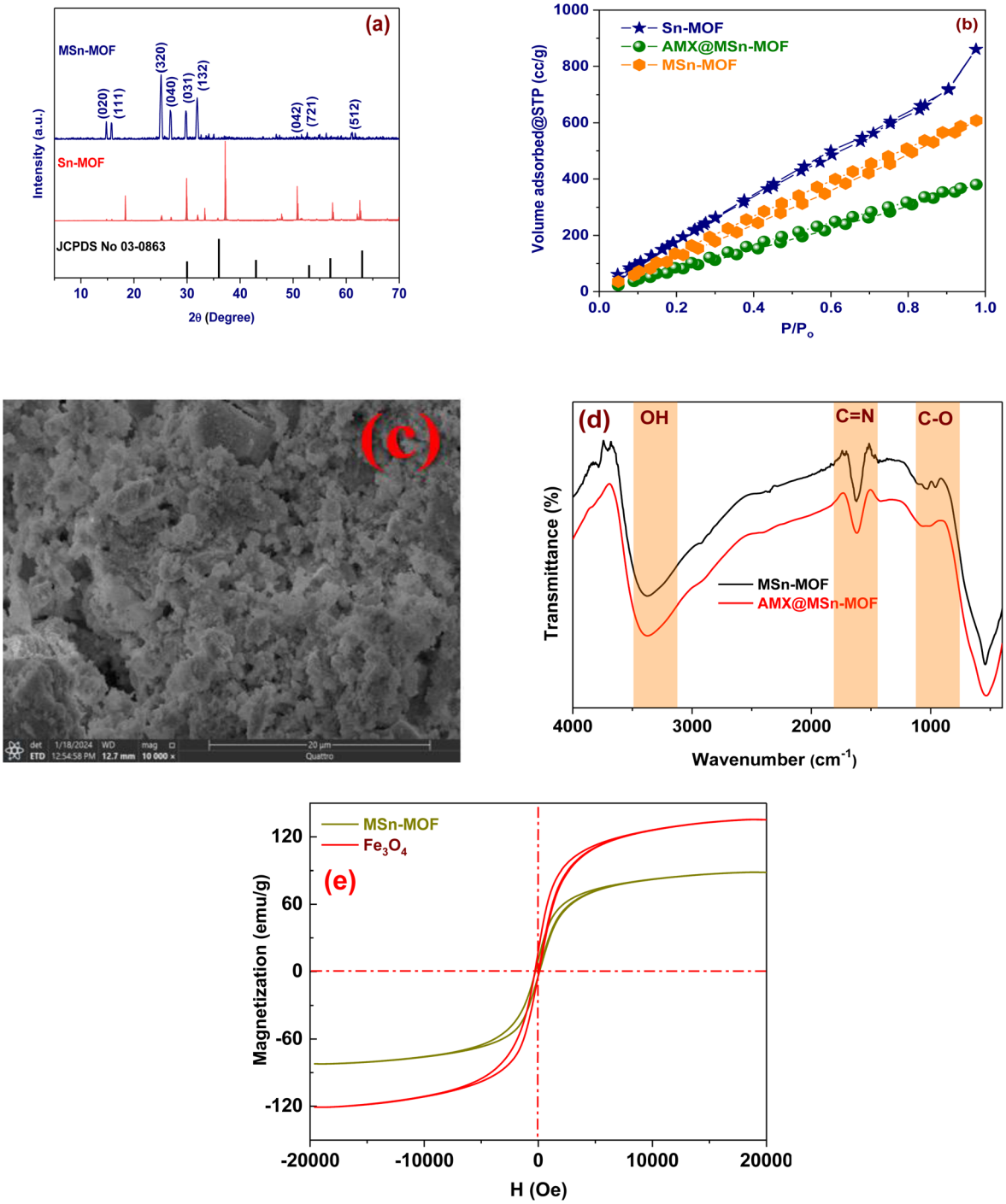

Fig. 2 (a) XRD, (b) BET, (c) SEM, (d) FT-IR, and (e) magnetization of MSn-MOFs.

regulate the adsorption process, which is significantly pH-dependent. According to the pH of the solution, AMX displays several forms (Fig. 4(a)). It exhibits a noticeable cationic tendency for pH < pK_a^1 = 2.4 (NH_2 protonated), zwitterionic among pK_a^1 and pK_a^2 = 7.4 (NH_2 protonated, COOH deprotonated), and anionic among pK_a^2 and pK_a^3 = 9.6 (COOH deprotonated). Furthermore, it displays a greater negative charge at pH values higher than 9.6 (both versions, COOH as well as OH deprotonated). The PZC of the MTM was 7.5 with respect to the adsorptive surface. It is important to note that MSn-MOF plays a vital role in refining the adsorption procedure because it prevents aggregation, provides thermal stabilization, and significantly growth of the quantity of adsorption sites.[37–39] The positively charged surface of MSn-MOF, which is located beneath its PZC, is electrostatically attracted to NH_3^+ when the pH is below pK_a^1 and AMX is in its cationic state. Even so, Fig. 4(b) shows high adsorption efficiency in this area, suggesting that driving forces other than electrostatic contact are at

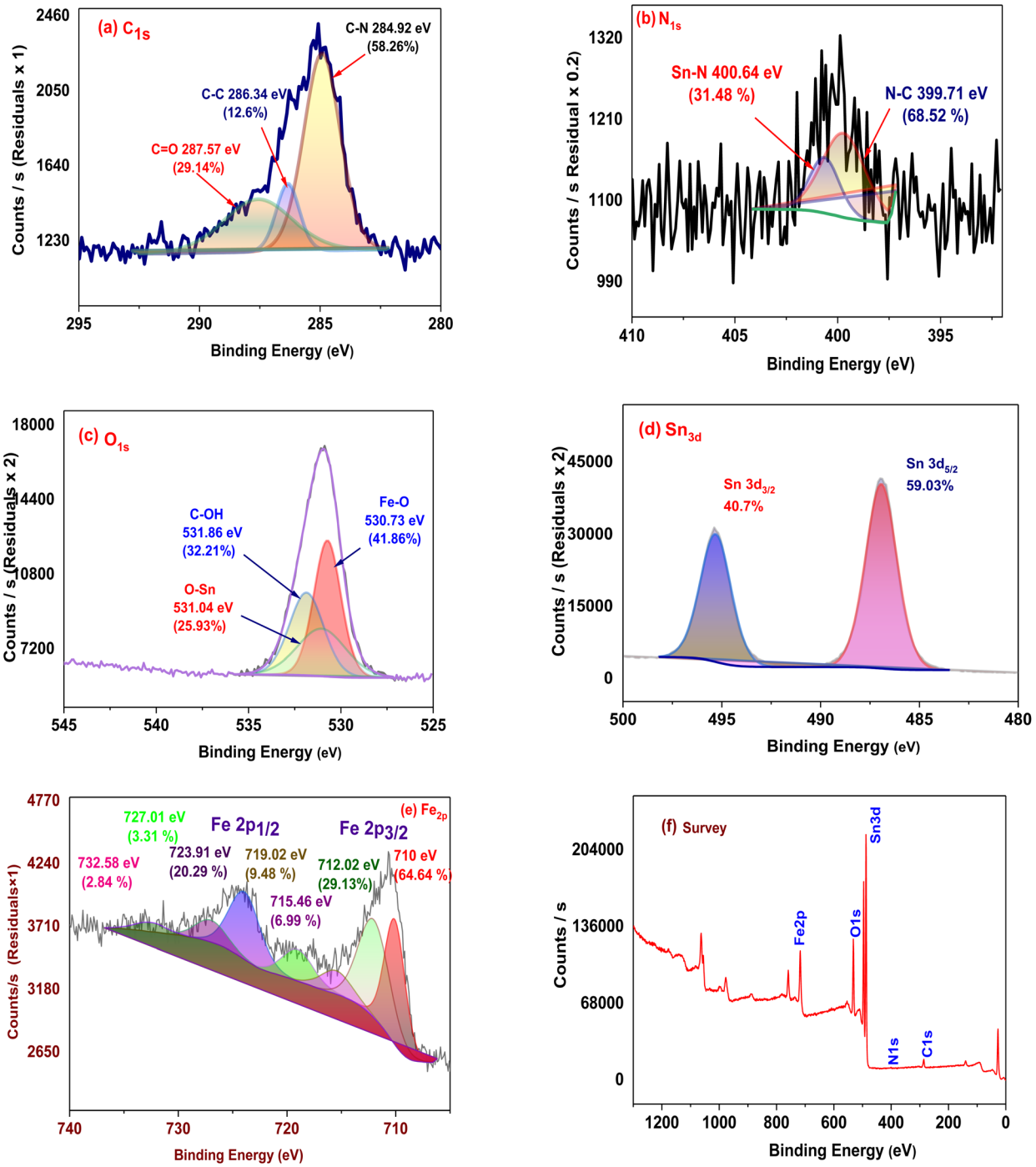

Fig. 3 Analysis of MSn-MOFs (a–f) using X-ray photoelectron spectroscopy (XPS).

play. When the pH falls between the standards of pK_a^1 and PZC, the adsorbent surface has a positive charge, whereas AMX primarily occurs in its zwitterionic method, while a small proportion of cationic and anionic AMX exist for pH values greater than pK_a^1 and less than pK_a^2, respectively. The electrostatic attraction between the positively charged surface and the carboxylate anion (COO^-) is the primary driving force inside this range, thereby aiding in the adsorption procedure. This observation aligns with the optimal adsorption efficacy varieties illustrated in Fig. 4(c). In the investigation of AMX adsorption onto MSn-MOF, pH is important because it may have an impact on the surface charge of the adsorbent besides the charge or molecular form of the adsorbate. To get the maximum efficiency of adsorption at given concentrations of AMX of 2.6×10^{-3} mmol L^{-1} and 0.02 g of adsorbent, the impact of pH was examined in the range of 1–12. According to the findings in Fig. 4(c), pH 6 results in the highest maximal adsorption capacity. The studies worked best at a pH of 6, which is a neutral pH that does not require adjustment, according to the findings. For pH values between PZC and pK_a^3, the adsorbent surface

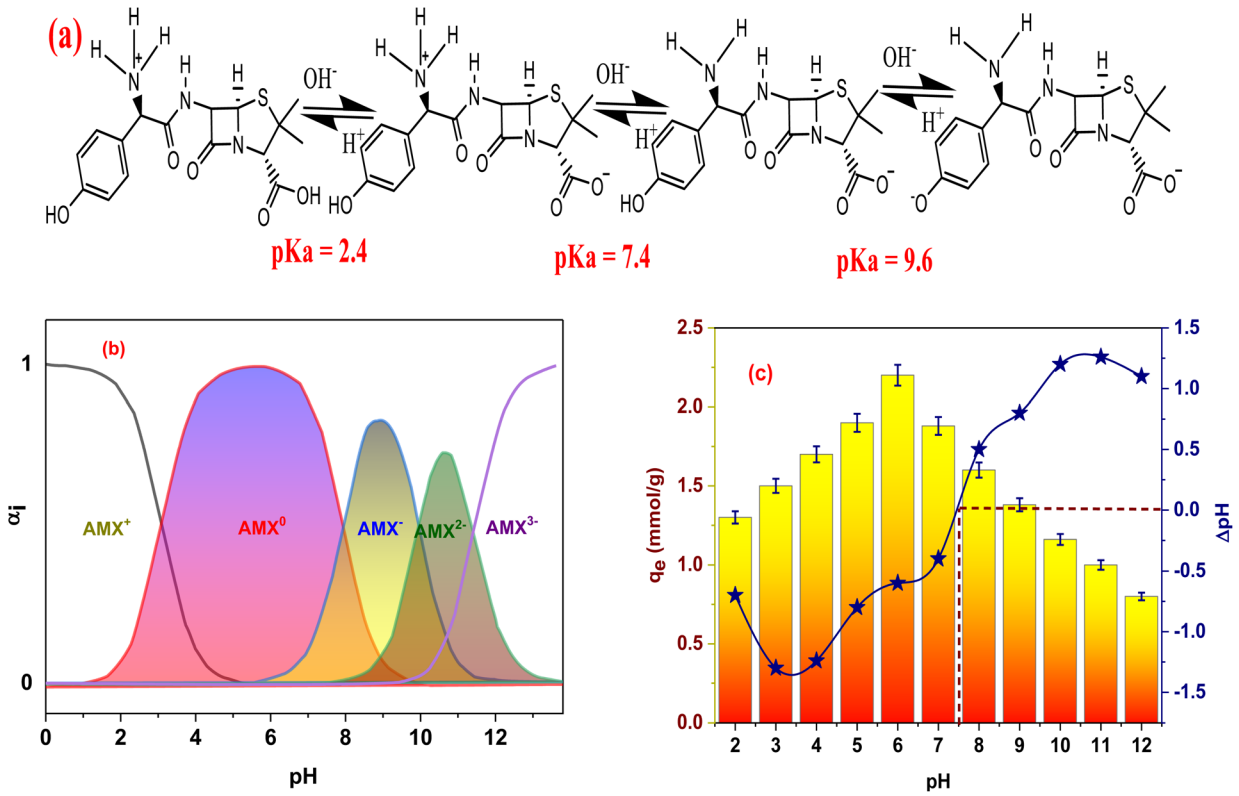

Fig. 4 (a) The effect of pH on the structural change of AMX, (b) pH species, and (c) change in the adsorption capacity.

acquires a negative charge, and the anionic form of AMX becomes predominant, resulting in electrostatic repulsion between AMX and MSn-MOF. This trend remains valid for pH values greater than pK_a[3], wherever AMX exhibits advanced negative charge, consequently diminishing the complete adsorption efficacy. The influence of cation–π interactions in these regions is not significant since it diminishes as the pH rises. The removal approach is highly successful for large concentrations of AMX in water, as seen by Fig. 4(c), and it has great removal effectiveness throughout the entire pH range.[31,40]

3.2.2. Result of dose. Examining the effects of adsorbent dose was crucial to figuring out the least quantity of adsorbent needed to guarantee maximal adsorption capability. Additionally, this would lower the expense of the adsorbent per amount of antibiotic solution that needs to be handled. Fig. S1 (ESI)† displays the impact of changing the quantity of the adsorbent (m) from 0.02 to 0.25 g on equilibrium adsorption capacity (q_e). The elimination efficiency of AMX by MSn-MOF rose quickly when m was elevated, reaching maximum values of 97.7 percent. However, q_e reduced when m was greater than 0.02 g, most likely because fewer available adsorption sites meant that more of them were exposed to antibiotics.[26,38,39] The study's findings on the impact of MSn-MOF concentration showed that the effectiveness of removal increased with MSn-MOF dosage. At lower dosages, this increase occurs faster, and the concentration progressively increases with a greater gradient. It can be the result of both an increased surface area and an increased number of adsorption sites. The results show that biomass has a higher capacity for adsorption at low levels of MSn-MOF than at high values. The existence of active unsaturated sites for organic bonds may explain the greater adsorption ability at small adsorbent doses (Fig. S1(a)†).

3.2.3. Effect of AMX concentration. The starting AMX concentration additionally impacts the clearance efficiency when using different AMX doses at pH 6. The dosage of AMX was increased, and the drug's adsorption sites increased. A higher concentration results in more molecules interacting with the MSn-MOF surface, thus increasing the quantity of AMX that can be adsorbed. Although there were several viable locations for adsorption in the adsorbent, which were adequate to completely and successfully absorb AMX at the reduced initial AMX concentration, this caused considerable elimination rates. But as the AMX concentrations increased, the substance's surface included less easily accessible locations for adsorption, and the ones that remained were not large enough to bind AMX (Fig. S1(b)†).[33]

3.2.4. Effect of contact time and temperature. The impact of the duration of contact, which varied from 5 to 100 minutes, on AMX adsorption was investigated. The results we obtained demonstrate that AMX removal increased with time and saturates at 100 minutes. The findings show that AMX sorption is relatively high during the first hour of adsorption, which could be attributed to the large surface area and active center obtainability of MSn-MOF.[33] The effective adsorption can also be attributed to these properties. The AMX sorption rate stabilized as the porous MSn-MOFs and active sites were depleted (Fig. S1(c)†).

3.2.5. Effect of temperature. The discoveries of the study on the impact of temperature on MSn-MOF's capacity to adsorb AMX are shown in Fig. S1(d).† There was an indication towards an increase in the capability for the adsorption of MSn-MOF on AMX when the operation temperature was elevated from 20 to 50 °C. Only a small change in the adsorption capacity was seen after raising the temperature to 50 °C. The pattern and increase in AMX's capacity for adsorption at elevated temperatures were the same.[41]

3.3. Adsorption isotherm

When researching the adsorption of a certain material onto a particular adsorbent, using adsorption isotherm models can have a number of benefits. Let's think about how AMX, a generic name for an antibiotic, adheres to MSn-MOF here (a generic term for a specific adsorbent). Adsorption isotherm models have a number of advantages over Langmuir, Freundlich, Temkin, Khan, Dubinin–Radushkevich, Toth, and Jovanovic in this situation, including understanding the mechanism of AMX adsorption onto MSn-MOF, which can be aided by adsorption isotherm models. It is possible to fit data from experiments to the proper isotherm model and establish whether the process of adsorption is monolayer or multilayer.[42] Adsorption isotherm models provide the quantitative description of the adsorption process. These models offer variables, such as the maximum adsorption capacity, equilibrium constant, and surface area coverage, that can describe the affinity of AMX for the MSn-MOF surface. It is feasible to compare the performance of MSn-MOF with other adsorbents for AMX adsorption using several adsorption isotherm models. In contrast to other prospective adsorbents, this comparison can assist establish the efficacy and suitability of MSn-MOF for the elimination of AMX from solution. Adsorption isotherm models can help with the adjustment of adsorption settings. Understanding the behavior of adsorption makes it possible to tune variables like pH, temperature, beginning concentration, and contact time to maximize the adsorption efficiency and reduce cost and energy use. Adsorption isotherm models can be used to forecast how AMX will behave as it adsorbs onto MSn-MOF under various operating conditions, giving information about how these changes may impact the adsorption capacity and efficiency. For creating effective and affordable adsorption methods, this predictive skill is essential. The cogency of the selected model can be assessed by relating the experimental data with the predicted data from the adsorption isotherm models. The credibility of the study results is increased by confirming that the chosen model appropriately depicts the adsorption behavior of AMX onto MSn-MOF through this validation. Overall, the use of adsorption isotherm models can significantly improve our knowledge, ability to predict, and ability to optimize the adsorption process. This knowledge can be extremely useful in designing and operating effective adsorption systems for the removal of AMX using MSn-MOF as the adsorbent.

For modelling the adsorption of an AMX onto the surface of MSn-MOF, one of the most popular models is the Langmuir adsorption isotherm. It was formulated in 1918 by Irving Langmuir and is predicated on the following premises: on the adsorbent surface, adsorption occurs at certain homogenous locations. The adsorbent's surface is uniform and energetically homogenous; thus, the adsorption of one molecule has no bearing on the adsorption of other molecules (Fig. 5). As stated by the Langmuir isotherm, the adsorption procedure creates a monolayer on the surface, and the rate of adsorption is constrained by the number of places on the superficial. The Langmuir isotherm is helpful for comprehending how adsorption behaves at low concentrations and can offer important insights into the adsorbent's adsorption capacity and surface coverage.[33] At large solute concentrations or when multilayer adsorption takes place, it might not, however, sufficiently represent the adsorption procedure. The maximal adsorption capability and the energy of adsorption can be calculated from the experimental data by fitting it to the Langmuir equation once the Langmuir isotherm is practical to the adsorption of AMX onto MSn-MOF. This can be used to comprehend the effectiveness and capacity of MTM for the removal of AMX and to forecast how the adsorption process will behave under various circumstances (Fig. 5(a)). Another popular empirical model for modelling adsorption on a heterogeneous surface is the Freundlich adsorption isotherm model, which Herbert Freundlich introduced in 1906. The Freundlich isotherm does not presume monolayer adsorption or suggest specific sites for adsorption, unlike the Langmuir isotherm. It works for multilayer adsorption. According to the Freundlich isotherm, adsorption is a reversible process, and as the solute concentration rises, the adsorption capacity of the adsorbent also increases. The value of n gives information about the favorability of adsorption; normally, a value of n among 1 and 10 designates a favorable adsorption; in this case, the value was 6.02, indicating a favorable adsorption process. This model can be used in situations where the adsorbate forms many layers on the surface and where the energy is distributed in a variety of ways on the adsorbent surface. However, the adsorption of AMX onto MSn-MOF was fitted to Langmuir rather than Freundlich model, which suggested that the adsorption was monolayer (Tables S2 and S3, ESI†).

The adsorption of AMX particles onto a solid surface of MSn-MOF is theoretically defined by the Dubinin–Radushkevich (DR) adsorption isotherm model. The model presupposes that the exponential function of the isosteric heat of adsorption is connected to the adsorption potential energy of a molecule in the micropores of a solid surface. When it comes to microporous materials, where the majority of the adsorption takes place inside very small pores, the DR isotherm model is particularly useful. This model has been used to examine and forecast the adsorption behavior of gases and vapors on porous materials in a number of disciplines, including surface chemistry, material science, and environmental science. The features of various adsorbents and their uses in gas separation, purification, and catalysis have also been made clear by this. The adsorption method in this instance was chemisorption, and the adsorption energy was 20.4 kJ mol^{-1}. The Temkin adsorption isotherm is a model used to describe the adsorption of particles on a solid surface. It considers the interactions among the adsorbate with

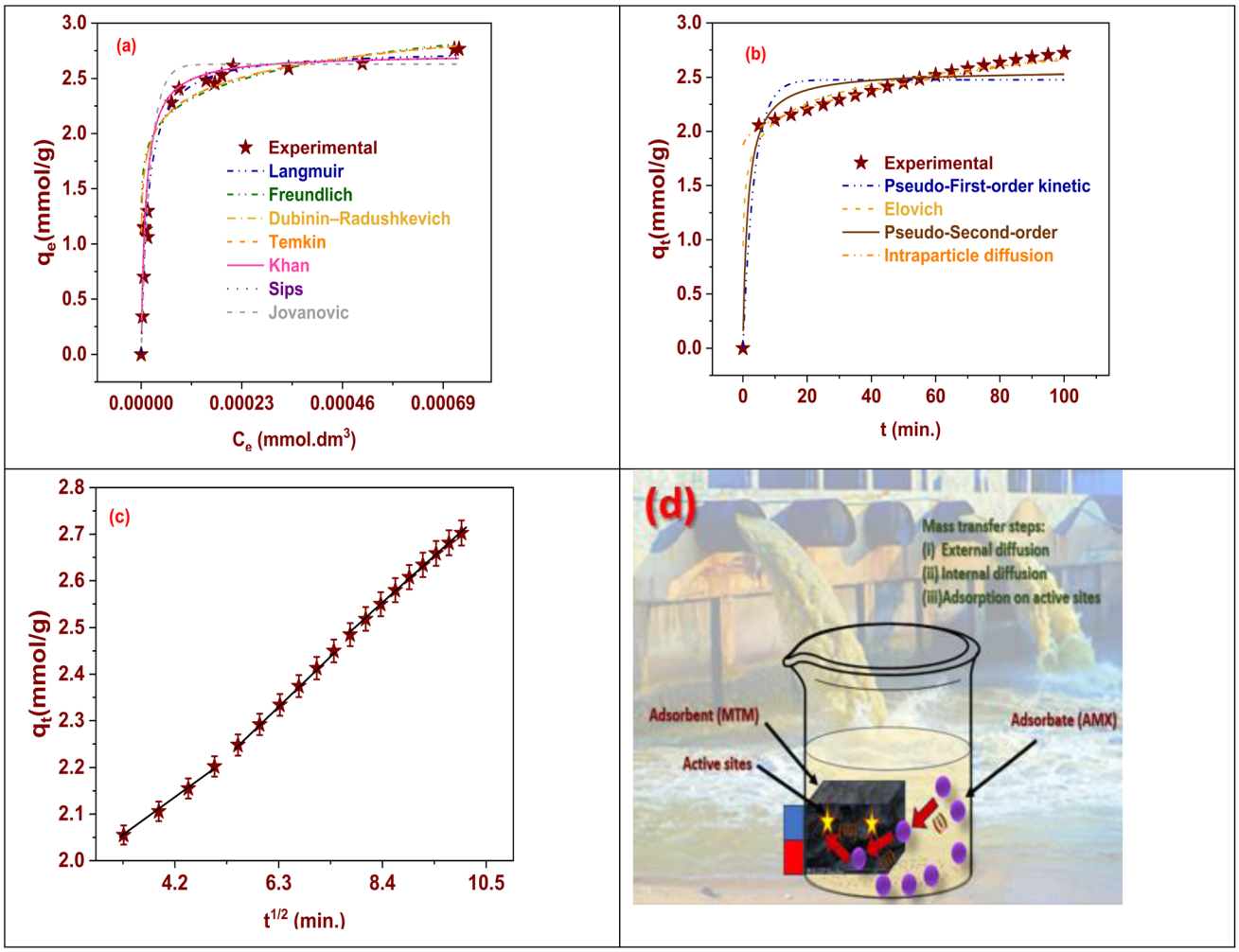

Fig. 5 (a) Adsorption isotherm model, (b) adsorption kinetic models, (c) IPD model, and (d) schematic diagram of adsorption of AMX onto MSn-MOFs.

a solid surface, supposing that adsorbent–adsorbate contacts lead to a decline in the heat of adsorption of all atoms in the layer, which is assumed to be linear. The claim that the heat of adsorption is constant, on the other hand, is characterized by the Langmuir adsorption isotherm. The Temkin isotherm makes the assumption that all molecules in the layer's heat of adsorption will drop linearly with attention as a result of adsorbent–adsorbate interactions. Since the Langmuir model assumes a constant heat of adsorption, this makes it a more inclusive model. It's critical to keep in mind that the Temkin isotherm is an experimental equation and might not be able to fully explain the adsorption procedure at the molecular level. The Temkin isotherm has found use in several fields, including surface chemistry, material science, and catalysis, and consider the interactions among adsorbates and solid surfaces.[43]

The adsorption of AMX onto solid surfaces using MSn-MOF is expressed by the Toth adsorption isotherm. When there is significant adsorbate–adsorbate interaction and when the process of adsorption occurs on surfaces through different energies, the Toth isotherm is frequently used. In particular, on heterogeneous surfaces, the Toth isotherm is adaptable and may explain a variety of adsorption events, including both physical and chemical adsorption. Its applications have been discovered in the characterization of porous materials. While the Jovanovic model also relies on the Langmuir model's underlying assumptions, it takes into consideration the possibility of specific mechanical interactions arising among the adsorbent with the adsorbate (Table S2, ESI†). Finally, from Table S2† and Fig. 5(a), it can be postulated that the Langmuir adsorption isotherm was the best fitted model, and the adsorption procedure was the chemisorption as the adsorption energy was 20.62 kJ mol^{-1}. The Langmuir adsorption isotherm represented the best-fitting model, according to Table S2† and Fig. 5(a); the adsorption mechanism was chemisorption, as indicated by the adsorption energy of 20.62 kJ mol^{-1}.

3.4. Adsorption kinetics

There are several advantages to using adsorption kinetic models, such as pseudo-first order, pseudo-second order, Elovich, and intraparticle diffusion when researching processes for adsorption. According to the pseudo-first order model, the rate

of adsorption is corresponding to the difference between the adsorbate's initial and equilibrium concentrations. It is possible to find the initial adsorption rate and the rate constant using this method. The rate of adsorption is inversely related to the square of the variance among the equilibrium and beginning levels of the adsorbate, as per the pseudo-second order model. This model permits for the resolution of the adsorption procedure, the equilibrium capacity for adsorption, and the rate constant.[27] Compared to the pseudo-first order model, the model is more commonly used since it is believed to be more precise at explaining the procedure of adsorption. The Elovich model states that the rate of adsorption gradually decreases as the adsorbent surface sites for adsorption become saturated. The rate of adsorption is controlled by the adsorbate's intraparticle diffusion through the adsorbent's porosity. This model is able to calculate the constant rate of intraparticle diffusion as well as the thickness of the barrier layer encircling the adsorbent nanoparticles. Considering the mechanism of adsorption and the factors affecting the adsorption rate are additionally aided by the model (Table 1).

It is also crucial to look at how treatment time affects the adsorbent–adsorbate interaction procedure in order to calculate the adsorption rate as well as its leading phase. A quicker ability of adsorbate removal in the former stage is shown in Fig. 5(b), which clarifies the impact of interaction time on AMX removal by MSn-MOF. The reason for this increased competence is that AMX molecules migrate (mass transfer) through the bulk solutions to the open adsorptive sites on the adsorbent surface more quickly. Following that, a gradual decrease in processing capacity was observed as the process of adsorption went on; at about 100 minutes, the equilibrium stage was achieved and no detectable adsorption took place. Within 100 minutes, the sorbed AMX molecules' saturation (lack) of MSn-MOF adsorptive locations made the adsorption procedure inconsequential.[37] The PFORE, PSORE, IPD, and Elovich models were used to evaluate the time taken for the interaction impact and its order as a function of adsorption kinetics, which represented the AMX diffusion procedure and their controlling step. According to PFORE, there is a direct proportionality among the rate of adsorption and the variation in q_e and q_t. The linearized and non-linear fitting was applied for accurate model suitability assessment, as shown in Fig. 5(b). Considering the estimated R^2 presented in Table 1 for the specified models makes it easy to infer that the PSORE model fit the results of AMX adsorption over MSn-MOF.[44]

Table 1 Adsorption kinetic parameters of adsorption of AMX onto MSn-MOFs

Model	Adsorption parameter	Value
Pseudo-first-order kinetic	K_1 (min^{-1})	0.2828
	q_e (mmol g^{-1})	2.48
	Reduced chi-sqr	0.03167
	Residual sum of squares	0.60175
	R-square (COD)	0.90735
	Adj. *R*-square	0.90248
	R^2	0.03167
Pseudo-second-order kinetic	K_2 (g mg^{-1} min^{-1})	0.25392
	q_e (mmol g^{-1})exp	2.72
	q_e (mmol g^{-1})	2.68
	Reduced chi-sqr	0.01324
	Residual sum of squares	13.19923
	R-square (COD)	0.77777
	Adj. *R*-square	0.77755
	R^2	0.01324
Intraparticle diffusion	K_i (mg g^{-1} $min^{1/2}$)	0.083
	X (mg g^{-1})	1.84
	Reduced chi-sqr	0.03517
	Residual sum of squares	35.09682
	R-square (COD)	0.51886
	Adj. *R*-square	0.51838
	R^2	0.03517
Elovich	β (g mg^{-1})	0.24844
	α (mg g^{-1} min^{-1})	1774.24809
	Reduced chi-sqr	0.00303
	Residual sum of squares	0.0576
	R-square (COD)	0.99113
	Adj. *R*-square	0.99066
	R^2	0.986

3.5. Diffusion mechanism

Hypothetically, the adsorbate has to move through three primary steps in order to move from the entire solution to the adsorbent surfaces: (i) in the initial stage, the AMX molecules from the majority of the solution are externally transported to the MSn-MOF surface (film diffusion); (ii) diffusion of AMX molecules into the adsorptive sites *via* the MSn-MOF pores is the second step (intraparticle diffusion); (iii) lastly, a strong bond formed between the anionic AMX particles and the positively charged MSn-MOF is associated with an even distribution of these molecules across the MSn-MOF surface. Employing the IPD model, we examined the rate-limiting stages of the AMX adsorption procedure. The procedure of adsorption on a porous adsorbent is composed of three main processes: mass transfer *via* the external liquid layer of the adsorbent, movement of the adsorbate molecule intraparticle, and adsorption on the interior or exterior sites of the adsorbent by chemical or physical bonding. Given that the last phase is assumed to be a speedy procedure, film or intraparticle diffusion is expected to donate the greatest amount to the adsorption rate. The IPD was adapted by graphing q_t *vs.* $t^{0.5}$ in order to understand the mechanism adsorption procedure. Three linear zones were the main behavior of the multi-linear graphs of q_t *vs.* $t^{0.5}$ in Fig. 5(c and d). It establishes that intraparticle diffusion did not seem to serve as the rate-limiting step for the overall adsorption procedure. The initial stage's larger rate constants may be explained by film diffusion happening on the MSn-MOF adsorbent's outside surface, which was followed by progressive intraparticle diffusion and, in conclusion, the equilibrium stage. Diffusion in meso- and micropores controls the uptake kinetics in the subsequent phases. The Elovich equation offers an additional visual representation of the variance in adsorption energies across adsorptive places, which is closely linked to their heterogeneous character.[45]

The application of several kinetic models can, in general, offer insightful information about the type of contact among

the adsorbent and the adsorbate as well as the adsorption mechanism. By contrasting the forecasts of the models with the outcomes of the experiments, researchers can determine the model that best matches the data. The relevant variables can then be used to forecast the adsorbent's effectiveness under different situations and enhance the adsorption conditions. Furthermore, using a variety of models can help to better understand the method of adsorption and aid in the interpretation of the experimental results (Table 1).

3.6. Adsorption thermodynamics

An improved understanding of the process can be obtained by seeing how altering the temperature affects the uptake of AMX and by examining the statistical changes made to the isothermal models. The target pollutant (AMX) molecules' mobility and the locations on the surface where they can settle are both hampered by this characteristic. Isotherm models allow for the analysis of variables at a fixed temperature, revealing new details about the mechanisms at play in the process, such as whether mono- or multi-layers are forming. This knowledge is essential for potential industrial-scale applications in the future, which frequently use constant variables. Understanding how changing the temperature affects the process's efficiency enables corrective actions to be taken to prevent financial losses. Different isothermal models are applied in the literature, allowing statistical limitations and the adsorbent's maximum capacity (q_{max}) to be estimated. This makes it easier to calculate the dosage required to achieve a particular efficiency. The optimal performance should be at temperatures close to the environment when considering large-scale applications since this prevents a higher energy cost. Another aspect is that when conducting isothermal studies, it is possible to estimate the thermodynamic parameters. The standards of the Gibbs free energy fluctuations (ΔG°), entropy variations (ΔS°), and enthalpy value (ΔH°) are calculated using the estimation of these parameters. These metrics allow the researcher to learn more about the processes (physisorption/chemosorption) and type of process (exothermic/endothermic) involved. It has been confirmed that because most processes are more favorable at higher temperatures, the increase in adsorption temperature has a significant impact on the uptake of AMX. This supports the studies' ΔH° values, which provide good results supporting the endothermic nature of the process. The elimination of AMX from the water was found to be increased when the temperature was raised from 298 to 323 K.

Table 2 Thermodynamic limitation of adsorption of AMX onto MSn-MOF

Parameter	van't Hoff
Residual sum of squares	0.00239
Pearson's r	−0.99971
R-square (COD)	0.99941
Adj. R-square	0.99929
ΔH°	59.89
ΔS°	145.16

This research has utilized a wide variety of adsorbents. As can be observed in Table 2, $\Delta H^\circ > 0$ indicates that the adsorption process was endothermic, showing the significance that the removal efficiency increased with increasing temperature. Most of the manuscript's values of ΔS° were positive (above zero), indicating that the adsorbent had a high affinity for the adsorbate when considering entropic effects. This could be attributed to the adsorbent's release of hydration water molecules before they bonded with the adsorbent surface.[46] A decrease in the degree of freedom is corroborated by negative values, which show more disordered systems (Fig. S2†).

3.7. Mechanism of interaction

We learn a little bit around the connections between the surfaces besides the AMX molecule when we examine the adsorption study parameters. However, using kinetic and isothermal models for particular interactions is insufficient. As a result, some investigations suggest adsorption mechanisms using thermodynamic parameters or FTIR analysis. The point of zero charge of the adsorbent (pH_{PZC}) and the measurement of the micro, meso, and macropores arranged on the surface are two further methods that can be used to better understand these interactions. Additionally, MSn-MOF's pH_{PZC} was 7.5. Therefore, it is advantageous that adsorption occurs at this pH because the positive charge on MSn-MOF's surface may attract the negative charge on AMX's surface. According to IUPAC, which proposed that materials with pore sizes between 2 and 50 nm might be categorized as mesoporous material, the adsorbent's 2.6 nm pore size indicated that it could be classified as a mesoporous material. The Dubinin–Radushkevich model's 20.6 kJ mol^{-1} adsorption energy indicates that the adsorption procedure was a chemisorption procedure. Furthermore, the FT-IR shifted functional group peak evidence supported the formation of the chemical bonds between MSn-MOF and AMX. Additional issues include the substance's chemical composition and a precise comprehension of the AMX equilibrium, which dictates whether the technique can proceed or not. Adsorption was endothermic and randomness existed between MSn-MOF and AMX, as evidenced by the thermodynamic characteristics that were examined (ΔH° was 59 kJ mol^{-1}, and both ΔH° and ΔS° were positive). However, it is anticipated that the AMX and the likely existence of the aromatic ring on the surface will cause n–π interactions to adopt the form of cation interactions.[47,48] Additionally, conventional hydrogen bonds between the adsorbent and neutral AMX are anticipated to develop. It seemed possible that some adsorption was occurring at the adsorbent's pores because both the surface area and the pore volume reduced after adsorption (Fig. 6).

3.8. Material recycling

As shown in Fig. S3(a),† for six cycles experiments, the removal efficiency of AMX were 98.6, 97.4, 96.88, 95.6, 93.2 and 91.6%, respectively. The removal effectiveness of the sixth recovery trial was still as high as 91.6 percent despite a 6.2 percent drop from the first experiment, showing that MSn-MOF had an adequate capacity for adsorbing AMX and was recyclable.[48,49] A little

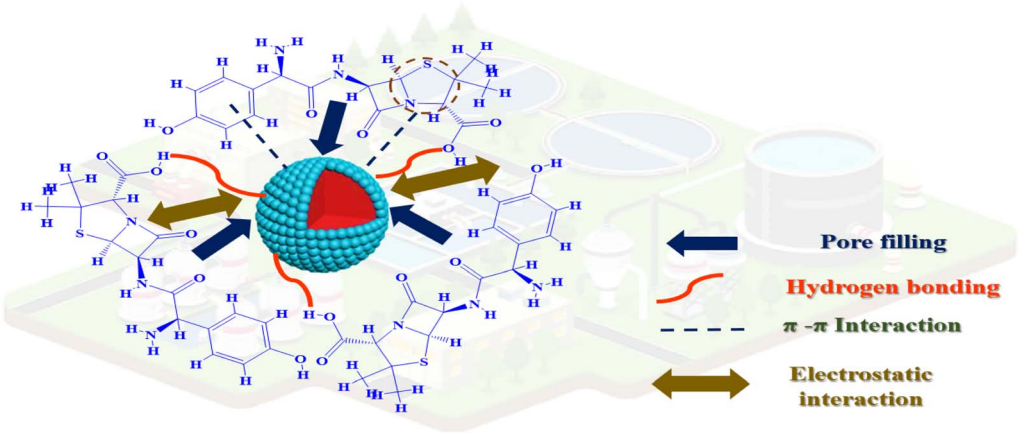

Fig. 6 Mechanism of interaction and adsorption of AMX onto MSn-MOFs.

amount of carbon deposits made from amoxicillin during the thermal regeneration of the exhausted MSn-MOF and filled in the pores of the regenerated MSn-MOF may be the cause of this drop. After every cycle, the adsorbent material was washed with NaOH or HCl until the pH reached 7. The functional groups on the MSn-MOF would have been worn out by ethanol washing. Thus, water and ethanol along with mechanical forces were used during various desorption procedures. On the other hand, the XRD analysis of the MSn-MOF's chemical stability revealed that the region of the functional groups did not vanish (Fig. S3(b)†).

3.9. Effect of interfering ions

Adsorption tests were carried out by adding NaCl to AMX solutions to study the impact of ionic strength; the absorption capacity *versus* the concentration of NaCl clearly demonstrates that its presence significantly reduces the adsorption capacity (Fig. S4†). This is a result of the struggle between Na^+, Cl^-, and AMX molecules, and in this situation, the surface chemistry is crucial to the adsorption of AMX. A few possible mechanisms, like complexation and electrostatic interaction, have been hypothesized in light of AMX's chemical makeup and adsorbent characteristics. As AMX and MSn-MOF molecules can both be protonated and deprotonated, they are electrostatically pulled to each other and the adsorbents with opposite charges. Since the initial pH and the presence of a strong electrolyte like Na^+ or Cl^- have a noteworthy impact on the AMX adsorption onto the adsorbent, electrostatic contact is probably the predominant mechanism for AMX adsorption.[50]

3.10. In contrast to alternative adsorbents

The highest sorption abilities of the MSn-MOF sorbent are compared including several values from the scientific literature (Table S4, ESI†). The direct assessment of sorption effectiveness is difficult because of diverse experimental arrangements, but this is a useful criterion for estimating these materials' possibilities in general. It is vital to emphasize that the quick kinetics of the bivalve shell sorbent is a significant benefit. The MSn-MOF's strong sorption capacity for AMX suggests that the sorbent may hold promise for actual usage in the elimination of AMX from wastewater.[51,52]

3.11. The checking of statistical analysis and model fitting

BBD is one of the RSMs used to study the relationships between numerous independent variables. We picked BBD for this study because it is simple and can reduce the number of experiments, requiring fewer levels. Up to 17 tests have been performed, and the results of these experiments have been used to estimate the response surface and determine AMX's ideal adsorption capacity. The response parameters state that the independent variables in Table S5† determine how much adsorption capacity is obtained (q_e). The findings of this study suggest that AMX adsorption involves interactions between several variables. Therefore, it is important to understand the variables in this research that can have an impact that is statistically significant. The following eqn (3) explains the quadratic equation model.

$$q_e = 2.08 + -0.0122375 \times A + 0.676754 \times B + -0.104336 \times C + -0.005805 \times AB + -0.00776 \times AC + -0.0446925 \times BC + -0.0746488 \times A^2 + -0.172021 \times B^2 + -0.00837125 \times C^2 \quad (3)$$

With the equation represented in terms of coded factors, the response for specific instances of each element may be predicted. The high values of the factors are represented as +1 and the low levels as −1 by design. The comparative relevance of the elements might be ascertained utilizing the coded equation to compare the factor coefficients.

Eqn (4) might be used to represent the actual equation:

$$q_e = 1.02391 + (0.0424609 \times A) + (0.0235285 \times B) + (-0.212357 \times C) + (-2.44421 \times 10^{-5} \times AB) + (-0.0134957 \times AC) + (-0.00818169 \times BC) + (-0.00298595 \times A^2) + (-7.62421 \times 10^{-5} \times B^2) + (-0.632987 \times C^2) \quad (4)$$

The response for certain levels of each variable can be predicted as the equation is expressed in terms of the real factors. Every factor's values in this case should be expressed in the

Table 3 Statistical overview of the various AMX adsorption models over MSn-MOF models

Source	Std. dev.	Sequential *p*-value	Press	Adj R^2	Pred R^2	Remark
Linear	0.1141	<0.0001	0.2851	0.9468	0.9273	
2F1	0.1269	0.9121	0.5385	0.9343	0.8627	
Quadratic	**0.0261**	**<0.0001**	**0.0762**	**0.9972**	**0.9806**	Suggested
Cubic	0.0000			1.0000		Aliased

initial units. Considering that the coefficients of this equation have been modified to account for the units of every element and the intercept is not precisely in the center of the design space; this formula should not be used to assess the relative importance of each factor. An investigation of adjustment (ANOVA) is carried out in the batch experiments using MSn-MOF adsorbent to adsorb AMX to demonstrate crucial criteria in certification modelling and discover significant factors and interactions that affect AMX adsorption. Researchers frequently use ANOVA to define interactions between the process and response variables in data visualization. The *p*-value column displays the significance of the *F*-value based on the quantity of degrees of freedom (DF) in the model. Significant impacts are most evident with larger *F*-values and lower *P*-values (Prob $\gg$ *F*). The interaction of components is significant when the probability value is *p* 0.05, allowing for a more precise and fault-free modelling of the experiment. The results of the ANOVA analysis are shown in Table S6.†

The parameters utilized to indicate whether the findings of the statistical model may be used to analyze the actual data are shown in Table 3. The outcomes of ANOVA for a adsorption capacity showed that the R^2 value was 0.9988 and adj-R^2 was 0.9972. An increased reliability of the model in predicting the adsorption capacity is indicated by a high R^2 value, which denotes good precision and correlation between experimental and predicted values. This shows that the fixed variables (pH (*A*), time (*B*), and dose (*C*)) have an effect of 2.75 mmol g^{-1} on the model. Based on Table 4, the models *F*-value, which is 639.39, can be seen. A *p*-value less than 0.05 specifies that the findings are meaningful. Due to noise, only 0.01 percent of cases may have an *F*-value this high. The quadratic model can also examine and assess how each factor interacts with the others. Terms from the model with a *P*-value of less than 0.0500 are deemed meaningful. In this case *A*, *B*, *C*, *BC*, A^2, and C^2 are significant model terms. If the number is more than 0.1000, the model terms are not meaningful. Model reduction may help if your model has a lot of extraneous terms (beyond those needed to maintain hierarchy). If the number of terms (excluding those required for endorsing the hierarchy) is not large, it is possible to decrease the quantity of terms in the model, allowing you to increase your model. The signal-to-noise ratio is measured with "adequate precision," where the target value is superior than 4. While the model's adeq-prec value is 87.72, this number indicates a sufficient signal for using the model to navigate the design chamber. Additionally, the relatively low coefficient of variation (0.857), which denotes a higher level of precision and better reproducibility in experimentation, is observed. The model's standard deviation is 0.026, demonstrating a strong connection between experimental results and prediction models. As a result, the constructed model yields precise and satisfactory results for the synthesis of biodiesel through the transesterification procedure. Table 4 demonstrated that the highest order polynomial should be utilized when the extra terms are important, and the model is not altered.

3.12. Response analysis for the adsorption capacity of AMX onto MSn-MOF

The response surface contour plot is the most effective way to illustrate how different parameters affect the experimental outcomes that were being studied. Design-Expert software (version 13.0.5) was used to create the response surface equation contour plot for the purpose of studying the impacts of variable interactions on the ability of AMX to adsorb onto MSn-MOF. Fig. 7 shows the effects of pH, time, besides adsorbent dose on the ability of AMX to be removed from the aqueous solution by adsorption.

The relationship between the adsorption of AMX accomplished by three separate parameters is depicted in Fig. 7 using 2-D and 3-D models: pH (*A*), time of interaction (*B*), and dose (*C*). Fig. 7 depicts the development of a 2-D and 3-D response surface plot to demonstrate the interaction among pH, time,

Table 4 Accumulation of squares for sequential modeling

Source	Sum of squares	d*f*	Mean squares	*F*-value	*P*-value	Remark
Mean *vs.* total	65.31	1	65.31			
Linear *vs.* mean	3.75	3	1.25	96.00	<0.0001	
2FI *vs.* linear	0.0084	3	0.0028	0.1732	0.9121	
Quadratic *vs.* 2FI	**0.1562**	**3**	**0.0521**	**76.51**	**<0.0001**	Suggested
Cubic *vs.* quadratic	0.0048	3	0.0016			Aliased
Residual	0.0000	4	0.0000			
Total	69.23	17	4.07			

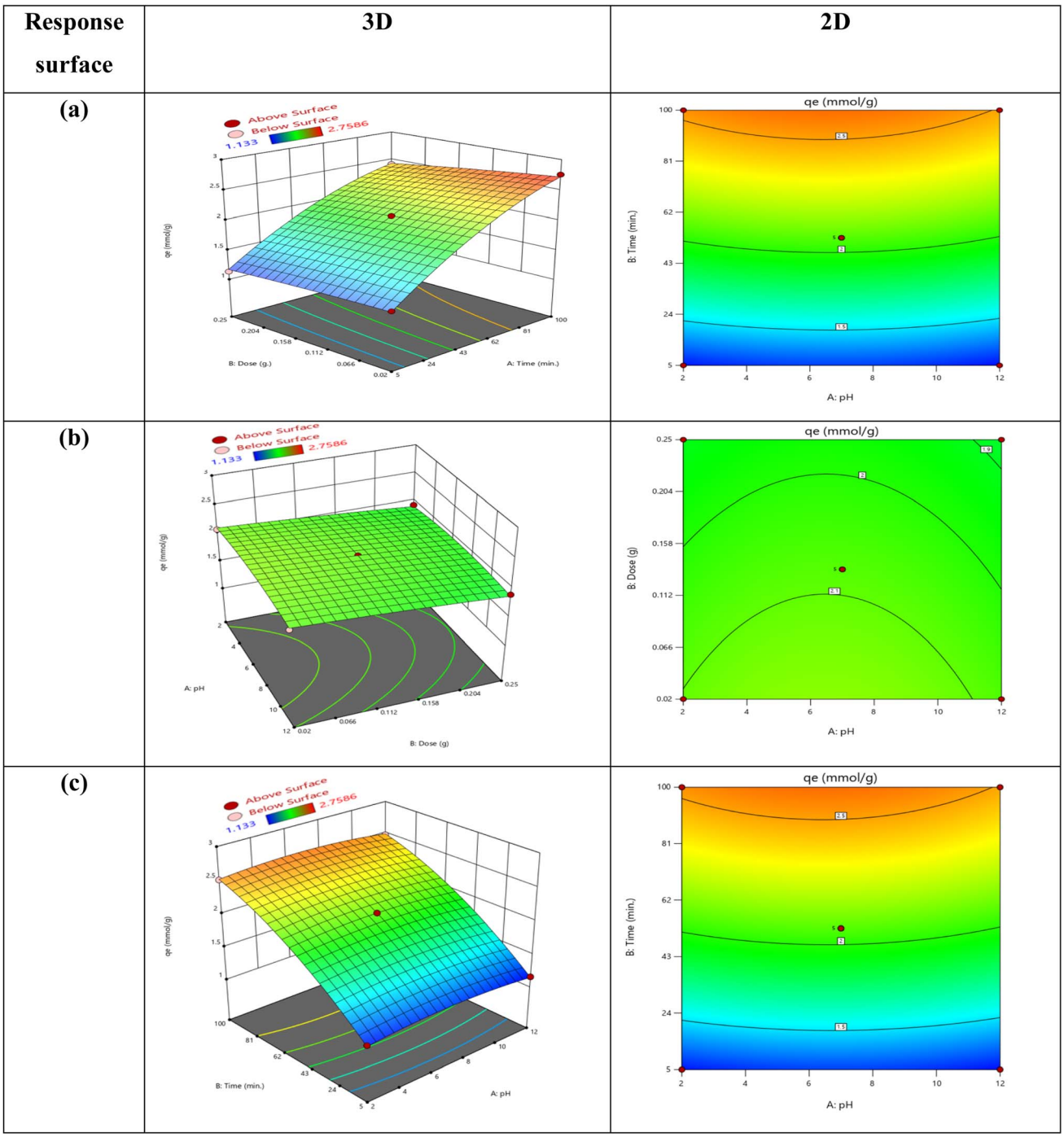

Fig. 7 Both 2D and 3D response surfaces.

and dose variations on the yield of adsorption capacity. First, longer contact times can enhance AMX's adsorption capacity. However, when the adsorbent dose is too high, the opposite occurs since the adsorbent's weight increases in a reversely proportional manner. Second, the adsorption capacity amplified with lower pH levels since it was practically determined that pH 6 is the ideal level. It also increased with lower adsorbent doses, and finally, the adsorption capacity increased with longer contact times.

3.13. Adequacy checking of the Box–Behnken model

Normally, checking for model adequacy is a requirement as part of model validation in order to confirm the model's accuracy and examine the analysis of investigational facts. An appropriate approach to the actual procedure will be provided by a sound and reliable mathematical model. Fig. S5† displays diagnostic graphs of the Box–Behnken model's suitability for transesterification-based biodiesel production. The presence of data points around the conventional line in Fig. S5(a)†

designates that the value is near to the projected value and that the model is highly reliable in forecasting the yield of adsorption capacity. This demonstrates how the model can strengthen the positive association between response variables to enable optimization. Externally studentized residuals in Fig. S5(b)† represent the differences between observed and projected values, split by their standard error. They can be viewed as standardized residuals. They aid in locating significant data points or outliers and are a crucial diagnostic tool in regression analysis. After taking into consideration the influence of other data points, the connection between externally studentized residuals and anticipated values in a regression analysis shows how much individual data points depart from the expected values of the overall model. One can learn more about the general pattern of the residuals, identify potential outliers, and evaluate the overall model fit by looking at this relationship. Understanding how the residuals evolve over the course of the observations or experimental runs is made easier by looking at Fig. S5(c and d),† which shows the link between externally studentized residuals and the run number. This relationship enables the identification of any regular patterns or abnormalities that might be related to the order of the experimental runs while examining the experimental data. Any trends or patterns in the residuals that correspond to certain run numbers can be found by looking at the plot of externally studentized residuals against the run numbers. Such trends might point to recurring mistakes or irregularities in the data collection procedure, the experimental setup, or the measurement methods used throughout various trials. Finding these patterns is essential to guarantee the consistency and dependability of the experimental results. Additionally, the association between run numbers and externally studentized residuals aids in evaluating the general effectiveness of the experimental planning and execution. Understanding the underlying causes that may be affecting the experimental results can be gained by looking for any unexpected behavior or trends in the residuals with respect to the order of the experimental runs.

3.14. Perturbation and cubic models

The relationship between adsorption capacity and variations in pH and adsorption duration for AMX onto MSn-MOF is illustrated in Fig. S5(e).† Both the contour plot and the 3-D response surface plot have been employed to illustrate this relationship. It was soon evident that longer durations, lower adsorbent dosages, and lower pH levels all clearly increased the adsorption capacity. The optimal conditions for adsorption were specifically an acidic pH of 6, 0.02 g of adsorbent, and 100 minutes. Under these circumstances, the capacity for adsorption rose to 2.75 mmol g^{-1}. Each parameter is contrasted at a particular location in the well thought-out design space using the perturbation graph. Fig. S5(f)† displays the perturbation curve for the AMX adsorption capacity on MSn-MOF. All other parameters were kept constant and only one element was changed across its range to determine the yield response. The narrative highlights how time, dose, and pH are three key areas in the constructed environment that are impacted by each factor. All the components appear to have a favorable effect on the adsorption capacity. The perturbation graphic in Table 4, eqn (3) and (4) illustrates the significant curvature effect that time, pH, and dose have. The relationship between pH and the duration of the adsorption process shows how rapidly the adsorption capacity adjusted to these variables. The variable that was most important was determined by comparing the coefficients in eqn (4). The detected adsorption capacity response was positively impacted by the adsorption process's time, pH, and dosage in increasing amounts.[11]

3.15. Validation of the model

The purpose of the rechecking experiment was to contrast the actual value with the expected result under various extraction settings. The actual studies' results showed that the RSM model was correct because no discernible significant modifications ($p > 0.05$) were seen. The model of response was sufficient to represent the anticipated adsorption capacity condition, as evidenced by the good correlation between the real and expected findings. The optimal conditions were pH 6, dose of 0.02 g, and time of 100 minutes.[27,28] The optimal forecast point of maximum AMX adsorption capacity, according to Design-Expert 13.0, is roughly 2.75 mmol g^{-1}, and the corresponding ideal adsorption procedure limits are given in Fig. S6† (100 minutes of contact, pH 6.0, and 0.02 g of adsorbent).

4. Conclusion

According to the data, a highly effective adsorbent for amoxicillin (AMX) was created through the inclusion of pre-formed magnetite nanoparticles in the tin organic framework (MSn-MOF). Various methods have been used to characterize the adsorbent, including FT-IR, BET surface area, pH_{zpc}, SEM, XPS, and VSM. Under a variety of operational conditions, an experimental study of the adsorptive removal of AMX utilizing MSn-MOF has been conducted. The outcomes show that MSn-MOF has a significant adsorption capability of 2.75 mmol g^{-1} at an acidic pH of 6. The PSORE model, which is proportional to the Langmuir theory, has been used to fit the adsorption procedure onto MSn-MOF the best. Adsorption works through a number of methods, including n–π stacked molecules, hydrogen bonds, and electrostatic forces. At pH 6, 0.02 g of adsorbent per 25 mL, 250 rpm of agitation to lessen resistance to film diffusion, and equilibrium period of 100 min, the best sorption occurs. The sorption processes' thermodynamics predict exothermic adsorption, which fits the sorption isotherms quite well. Furthermore, MSn-MOF is reusable as evidenced by the fact that its desorption effectiveness is 91.6 percent after 6 successive cycles of adsorption/desorption. It has also been proven that using MSn-MOF to remove AMX from actual effluents works. Overall, the results point to the potential of MSn-MOF as a cost-effective and advantageous adsorbent for the treatment of AMX wastewater. MSn-MOF is a viable contender for wastewater treatment owing to its high adsorption capacity, reusability, and effectiveness. The removal of AMX and other pollutants from polluted water and wastewater can be done more affordably and

sustainably using MSn-MOF as opposed to conventional, expensive techniques of wastewater treatment.

Data availability

All relevant data are within the manuscript and available from the corresponding author upon request.

Conflicts of interest

The authors declare that they have no competing interests.

Acknowledgements

This research has been funded by Scientific Research Deanship at University of Ha'il-Saudi Arabia through project number RG-23 112. The authors highly appreciate and introduce deep thanks for Scientific Research Deanship University of Ha'il, Saudi Arabia.

References

1 I. Ali, Z. A. ALOthman and X. Mbianda, Preparation and characterization of nanoporous carbon for removal of amoxicillin antibiotic from water: Modelling, kinetics and thermodynamic studies, *Inorg. Chem. Commun.*, 2023, **155**, 111006.

2 J. Georgin, D. S. P. Franco, L. Meili, Y. Dehmani, G. S. dos Reis and E. C. Lima, Main advances and future prospects in the remediation of the antibiotic amoxicillin with a focus on adsorption technology: A critical review, *J. Water Process. Eng.*, 2023, **56**, 104407.

3 F. Edi-Soetaredjo, M. Slama, L. Sellaoui, H. Ghalla, M. B. E. H. Rhouma, S. Ismadji, B. Ernst, A. Bonilla-Petriciolet and A. B. Lamine, Highlighting the single and binary adsorption mechanism of amoxicillin and doripenem on copper benzene-1, 3, 5-tricarboxylate MOF via experiments, characterization, statistical physics modelling and DFT simulation, *Chem. Eng. J.*, 2023, **474**, 145633.

4 H. M. Nassef, G. A. A. M. Al-Hazmi, A. A. Alayyafi, M. G. El-Desouky and A. A. El-Bindary, Synthesis and characterization of new composite sponge combining of metal-organic framework and chitosan for the elimination of Pb(II), Cu(II) and Cd(II) ions from aqueous solutions: Batch adsorption and optimization using Box-Behnken design, *J. Mol. Liq.*, 2024, **394**, 123741.

5 P. Madariaga-Segovia, S. Párraga and C. A. Villamar-Ayala, Removal of triclosan, ibuprofen, amoxicillin and paracetamol using organic residues under a bibliometric-statistical analysis, *Bioresour. Technol. Rep.*, 2023, 101564.

6 W. A. El-Fattah, A. Guesmi, N. Ben Hamadi, M. G. El-Desouky and A. Shahat, A green synthesis of cellulose nanocrystals biosorbent for remediation of wastewater containing industrial dye, *Colloids Surf. A: Physicochem. Eng. Asp.*, 2024, **681**, 132729.

7 R. T. Mogharbel, K. Alkhamis, R. Felaly, M. G. El-Desouky, A. A. El-Bindary, N. M. El-Metwaly and M. A. El-Bindary, Superior adsorption and removal of industrial dye from aqueous solution via magnetic silver metal-organic framework nanocomposite, *Environ. Technol.*, 2023, DOI: **10.1080/09593330.2023.2178331**.

8 K. Yaghmaeian, G. Moussavi and A. Alahabadi, Removal of amoxicillin from contaminated water using NH4Cl-activated carbon: Continuous flow fixed-bed adsorption and catalytic ozonation regeneration, *Chem. Eng. J.*, 2014, **236**, 538–544.

9 A. M. Alsuhaibani, M. S. Refat, A. M. A. Adam, M. G. El-Desouky and A. A. El-Bindary, Enhanced adsorption of ceftriaxone antibiotics from water by mesoporous copper oxide nanosphere, *Desalin. Water Treat*, 2023, **281**, 234–248.

10 H. H. Alsharief, N. M. Alatawi, A. M. Al-bonayan, S. H. Alrefaee, F. A. Saad, M. G. El-Desouky and A. A. El-Bindary, Adsorption of Azorubine E122 dye via Na-mordenite with tryptophan composite: batch adsorption, Box–Behnken design optimisation and antibacterial activity, *Environ. Technol.*, 2023, DOI: **10.1080/09593330.2023.2219399**.

11 S. H. Alrefaee, M. Aljohani, K. Alkhamis, F. Shaaban, M. G. El-Desouky, A. A. El-Bindary and M. A. El-Bindary, Adsorption and effective removal of organophosphorus pesticides from aqueous solution via novel metal-organic framework: Adsorption isotherms, kinetics, and optimization via Box-Behnken design, *J. Mol. Liq.*, 2023, **384**, 122206.

12 H. El Farissi, A. Beraich, M. Lamsayah, A. Talhaoui and A. E. Bachiri, The efficiency of carbon modified by phosphoric acid (H_3PO_4) used in the removal of two antibiotics amoxicillin and metronidazole from polluted water: Experimental and theoretical investigation, *J. Mol. Liq.*, 2023, **391**, 123237.

13 S. Mirizadeh, C. Solisio, A. Converti and A. A. Casazza, Efficient removal of tetracycline, ciprofloxacin, and amoxicillin by novel magnetic chitosan/microalgae biocomposites, *Sep. Purif. Technol.*, 2024, **329**, 125115.

14 M. A. E. de Franco, C. B. de Carvalho, M. M. Bonetto, R. de Pelegrini Soares and L. A. Féris, Removal of amoxicillin from water by adsorption onto activated carbon in batch process and fixed bed column: kinetics, isotherms, experimental design and breakthrough curves modelling, *J. Cleaner Prod.*, 2017, **161**, 947–956.

15 J. Y. J. Yeo, D. S. Khaerudini, F. E. Soetaredjo, G. L. Waworuntu, S. Ismadji, J. Sunarso and S. Liu, Isotherm data for adsorption of amoxicillin, ampicillin, and doripenem onto bentonite, *Data Brief*, 2023, **48**, 109159.

16 S. S. Hussaini, M. Hussain, M. Asim, A. Al-Balushi, B. Al-Saidi, G. Al-Ghafri, M. Al Abri, N. Devunuri and K. Seku, Facial synthesis of an efficient magnetic composite adsorbent using multiwalled carbon nanotubes and frankincense resin for the removal of amoxicillin pharmaceutical pollutants, *J. Mol. Liq.*, 2023, **390**, 123166.

17 S. D. Al-Qahtani, M. Alhasani, N. Alkhathami, K. A. Abu Al-Ola, K. Alkhamis, M. G. El-Desouky and A. A. El-Bindary,

Effective levofloxacin adsorption and removal from aqueous solution onto tea waste biochar; synthesis, characterization, adsorption studies, and optimization by Box–Behnken design and its antibacterial activity, *Environ. Technol.*, 2023, DOI: 10.1080/09593330.2023.2283409.

18 A. Almahri, M. Morad, M. M. Aljohani, N. M. Alatawi, F. A. Saad, H. M. Abumelha, M. G. El-Desouky and A. A. El-Bindary, Atrazine reclamation from an aqueous environment using a ruthenium-based metal-organic framework, *Process Saf. Environ. Prot.*, 2023, **177**, 52–68.

19 A. Mojiri, M. Vakili, H. Farraji and S. Q. Aziz, Combined ozone oxidation process and adsorption methods for the removal of acetaminophen and amoxicillin from aqueous solution; kinetic and optimisation, *Environ. Technol. Innovation*, 2019, **15**, 100404.

20 P. Shi, C. Chen, X. Lu, P. Wang, S. Mi, J. Lu and Z. Tong, Preparation, characterization and adsorption potentiality of magnetic activated carbon from Eucalyptus sawdust for removal of amoxicillin: Adsorption behavior and mechanism, *Ind. Crops Prod.*, 2023, **203**, 117122.

21 V. Gadore, S. R. Mishra and M. Ahmaruzzaman, Bio-inspired sustainable synthesis of novel SnS2/biochar nanocomposite for adsorption coupled photodegradation of amoxicillin and congo red: Effects of reaction parameters, and water matrices, *J. Environ. Manage.*, 2023, **334**, 117496.

22 H. Laksaci, B. Belhamdi, O. Khelifi, A. Khelifi and M. Trari, Elimination of amoxicillin by adsorption on coffee waste based activated carbon, *J. Mol. Struct.*, 2023, **1274**, 134500.

23 A. A. Aryee, R. Han and L. Qu, Occurrence, detection and removal of amoxicillin in wastewater: A review, *J. Cleaner Prod.*, 2022, **368**, 133140.

24 M. Caravaca, Y. Vicente-Martínez, A. Soto-Meca and E. Angulo-González, Total removal of amoxicillin from water using magnetic core nanoparticles functionalized with silver, *Environ. Res.*, 2022, **211**, 113091.

25 Y. Gong, J. Yuan, Y. Pei, S. Liu and X. Luo, One-step quaternization and macromolecular reconstruction to prepare micro-/nano-porous cellulose beads from homogeneous solution for low-concentration amoxicillin removal, *Carbohydr. Polym.*, 2023, **315**, 120985.

26 T. A. Altalhi, G. A. M. Mersal, M. H. H. Mahmoud, T. Kumeria, M. G. El-Desouky, A. A. El-Bindary and M. A. El-Bindary, Adsorption of doxorubicin hydrochloride onto thermally treated green adsorbent: Equilibrium, kinetic and thermodynamic studies, *J. Mol. Struct.*, 2022, **1263**, 133160.

27 A. U. Khan, N. Malik, B. Singh, N. H. Ansari, M. Rehman and A. Yadav, Biosynthesis, and characterization of Zinc oxide nanoparticles (ZnONPs) obtained from the extract of waste of strawberry, *Umm Al-Qura Univ. J. Sci.*, 2023, **9**, 268–275.

28 V. S. Priya, S. K. Basha and V. S. Kumari, Kinetics and adsorption performance of biosorbent starch/poly(vinyl alcohol)/graphene oxide nanocomposite for the removal of dyes, *Umm Al-Qura Univ. J. Sci.*, 2023, **9**, 529–547.

29 A. Almahri, K. S. Abou-Melha, H. A. Katouah, A. M. Albonayan, F. A. Saad, M. G. El-Desouky and A. A. El-Bindary, Adsorption and removal of the harmful pesticide 2,4-dichlorophenylacetic acid from an aqueous environment via coffee waste biochar: Synthesis, characterization, adsorption study and optimization via Box-Behnken design, *J. Mol. Struct.*, 2023, **1293**, 136238.

30 M. M. Aljohani, S. D. Al-Qahtani, M. Alshareef, M. G. El-Desouky, A. A. El-Bindary, N. M. El-Metwaly and M. A. El-Bindary, Highly efficient adsorption and removal bio-staining dye from industrial wastewater onto mesoporous Ag-MOFs, *Process Saf. Environ. Prot.*, 2023, **172**, 395–407.

31 N. M. El-Metwaly, H. A. Katouah, M. G. El-Desouky, A. A. El-Bindary and M. A. El-Bindary, Fabricating of Fe_3O_4@Ag-MOF nanocomposite and evaluating its adsorption activity for removal of doxorubicin, *J. Environ. Sci. Health – Toxic/Hazard. Subst. Environ. Eng.*, 2022, **57**, 1099–1115.

32 M. A. El-Bindary, M. G. El-Desouky and A. A. El-Bindary, Adsorption of industrial dye from aqueous solutions onto thermally treated green adsorbent: A complete batch system evaluation, *J. Mol. Liq.*, 2022, **346**, 117082.

33 G. A. A. Al-Hazmi, A. A. El-Zahhar, M. G. El-Desouky and A. El-Bindary, Superior adsorption and removal of doxorubicin from aqueous solution using activated carbon via thermally treated green adsorbent: isothermal, kinetic, and thermodynamic studies, *Environ. Technol.*, 2022, DOI: 10.1080/09593330.2022.2159540.

34 M. G. El-Desouky, M. A. G. Khalil, M. A. M. El-Afify, A. A. El-Bindary and M. A. El-Bindary, Effective methods for removing different types of dyes – modelling analysisstatistical physics treatment and DFT calculations: a review, *Desalin. Water Treat*, 2022, **280**, 89–127.

35 M. G. El-Desouky, A. A. El-Bindary and M. A. El-Bindary, Low-temperature adsorption study of carbon dioxide on porous magnetite nanospheres iron oxide, *Biointerface Res. Appl. Chem.*, 2022, **12**, 6252–6268.

36 M. G. El-Desouky, A. Shahat, A. A. El-Bindary and M. A. El-Bindary, Description, kinetic and equilibrium studies of the adsorption of carbon dioxide in mesoporous iron oxide nanospheres, *Biointerface Res. Appl. Chem.*, 2022, **12**, 1022–1038.

37 G. A. A. Al-Hazmi, A. A. El-Zahhar, M. G. El-Desouky, M. A. El-Bindary and A. A. El-Bindary, Efficiency of Fe_3O_4@ZIF-8 for the removal of Doxorubicin from aqueous solutions: equilibrium, kinetics and thermodynamic studies, *Environ. Technol.*, 2024, **45**, 731–750.

38 A. S. Al-Wasidi, I. I. S. AlZahrani, H. I. Thawibaraka, A. M. Naglah, M. G. El-Desouky and M. A. El-Bindary, Adsorption studies of carbon dioxide and anionic dye on green adsorbent, *J. Mol. Struct.*, 2022, **1250**, 131736.

39 A. M. Alsuhaibani, M. S. Refat, A. A. Atta, M. G. El-Desouky and A. A. El-Bindary, Efficient adsorption and removal of tetracycline antibiotics from aqueous solutions onto nickel oxide nanoparticles via organometallic chelate, *Desalin. Water Treat*, 2022, **277**, 190–205.

40 D. Samir and C. Khemissi, Application of geothermometric and hydrochemical methods to the investigation of thermal water of sources in the Northeastern of Algeria case of Setif city, *Umm Al-Qura Univ. J. Sci.*, 2022, **8**, 69–78.

41 G. A. A. Al-Hazmi, A. A. El-Zahhar, M. G. El-Desouky, M. A. El-Bindary and A. A. El-Bindary, Adsorption of industrial dye onto a zirconium metal-organic framework: synthesis, characterization, kinetics, thermodynamics, and DFT calculations, *J. Coord. Chem.*, 2022, **75**, 1203–1229.

42 G. H. Al-Hazmi, M. S. Refat, M. G. El-Desouky, F. K. M. Wali and A. A. El-Bindary, Effective removal of industrial dye from aqueous solution using mesoporous nickel oxide: a complete batch system evaluation, *Desalin. Water Treat*, 2022, **273**, 246–260.

43 G. A. A. AlHazmi, K. S. AbouMelha, M. G. El-Desouky and A. A. El-Bindary, Effective adsorption of doxorubicin hydrochloride on zirconium metal-organic framework: Equilibrium, kinetic and thermodynamic studies, *J. Mol. Struct.*, 2022, **1258**, 132679.

44 M. G. El-Desouky, N. Hassan, A. Shahat, A. El-Didamony and A. A. El-Bindary, Synthesis and characterization of porous magnetite nanosphere iron oxide as a novel adsorbent of anionic dyes removal from aqueous solution, *Biointerface Res. Appl. Chem.*, 2021, **11**, 13377–13401.

45 M. G. El-Desouky and A. A. El-Bindary, Magnetic metal-organic framework (Fe3O4@ZIF-8) nanocomposites for adsorption of anionic dyes from wastewater, *Inorg. Nano-Met. Chem.*, 2021, DOI: **10.1080/24701556.2021.2007131**.

46 A. S. Al-Wasidi, I. I. S. AlZahrani, A. M. Naglah, M. G. El-Desouky, M. A. Khalil, A. A. El-Bindary and M. A. El-Bindary, Effective Removal of Methylene Blue From Aqueous Solution Using Metal-Organic Framework; Modelling Analysis, Statistical Physics Treatment and DFT Calculations, *ChemistrySelect*, 2021, **6**, 11431–11447.

47 S. S. Iqubal, Review on kinetic studies of α-hydroxy acids (glycolic, mandelic, citric, tartaric and malic) and some other organic compounds with water soluble nano particles of colloidal MnO_2 in absence and presence of non-ionic surfactant (TX-100), *Umm Al-Qura Univ. J. Sci.*, 2022, **8**, 79–84.

48 N. Hassan, A. Shahat, A. El-Didamony, M. G. El-Desouky and A. A. El-Bindary, Mesoporous iron oxide nano spheres for capturing organic dyes from water sources, *J. Mol. Struct.*, 2020, **1217**, 128361.

49 N. Hassan, A. Shahat, A. El-Didamony, M. G. El-Desouky and A. A. El-Bindary, Synthesis and characterization of ZnO nanoparticles via zeolitic imidazolate framework-8 and its application for removal of dyes, *J. Mol. Struct.*, 2020, **1210**, 128029.

50 H. A. Kiwaan, F. Sh. Mohamed, N. A. El-Ghamaz, N. M. Beshry and A. A. El-Bindary, Experimental and electrical studies of zeolitic imidazolate framework-8 for the adsorption of different dyes, *J. Mol. Liq.*, 2021, **338**, 116670.

51 S. S. Iqubal, Characterization, surface morphology and microstructure of water soluble colloidal MnO_2 nanoflakes, *Umm Al-Qura Univ. J. Sci.*, 2022, **8**, 33–36.

52 A. A. Alluhaybi, A. Alharbi, K. F. Alshammari and M. G. El-Desouky, Efficient Adsorption and Removal of the Herbicide 2, 4-Dichlorophenylacetic Acid from Aqueous Solutions Using MIL-88 (Fe)-NH_2, *ACS Omega*, 2023, **8**, 40775–40784.